ACS chemical biology

Articles

pubs.acs.org/acschemicalbiology

eZinCh-2: A Versatile, Genetically Encoded FRET Sensor for Cytosolic and Intraorganelle Zn^{2+} Imaging

Anne M. Hessels,[†] Pauline Chabosseau,[‡] Maarten H. Bakker,[†] Wouter Engelen,[†] Guy A. Rutter,[‡] Kathryn M. Taylor,[§] and Maarten Merkx*[,†]

[†]Laboratory of Chemical Biology and Institute of Complex Molecular Systems (ICMS), Department of Biomedical Engineering, Eindhoven University of Technology, Eindhoven, The Netherlands

[‡]Section of Cell Biology and Functional Genomics, Division of Medicine, Imperial College London, London, United Kingdom

[§]Breast Cancer Molecular Pharmacology Group, School of Pharmacy and Pharmaceutical Sciences, Cardiff University, Cardiff, United Kingdom

Supporting Information

ABSTRACT: Zn^{2+} plays essential and diverse roles in numerous cellular processes. To get a better understanding of intracellular Zn^{2+} homeostasis and the putative signaling role of Zn^{2+}, various fluorescent sensors have been developed that allow monitoring of Zn^{2+} concentrations in single living cells in real time. Thus far, two families of genetically encoded FRET-based Zn^{2+} sensors have been most widely applied, the eCALWY sensors developed by our group and the ZapCY sensors developed by Palmer and co-workers. Both have been successfully used to measure cytosolic free Zn^{2+}, but distinctly different concentrations have been reported when using these sensors to measure Zn^{2+} concentrations in the ER and mitochondria. Here, we report the development of a versatile alternative FRET sensor containing a *de novo* Cys_2His_2 binding pocket that was created on the surface of the donor and acceptor fluorescent domains. This eZinCh-2 sensor binds Zn^{2+} with a high affinity that is similar to that of eCALWY-4 (K_d = 1 nM at pH 7.1), while displaying a substantially larger change in emission ratio. eZinCh-2 not only provides an attractive alternative for measuring Zn^{2+} in the cytosol but was also successfully used for measuring Zn^{2+} in the ER, mitochondria, and secretory vesicles. Moreover, organelle-targeted eZinCh-2 can also be used in combination with the previously reported redCALWY sensors to allow multicolor imaging of intracellular Zn^{2+} simultaneously in the cytosol and the ER or mitochondria.

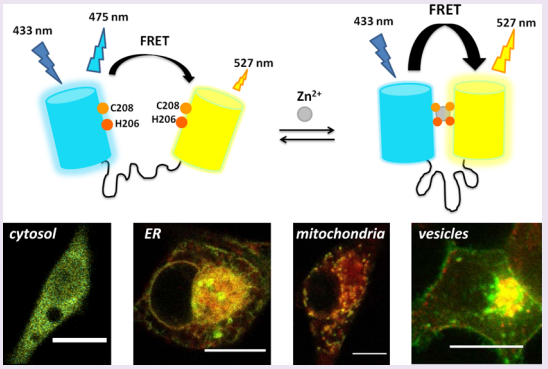

Although zinc is sometimes still referred to as a "trace metal ion", zinc ions play a range of essential roles in numerous cellular processes. In addition to serving as a cofactor in enzyme catalysis and protein stabilization,[1,2] Zn^{2+} ions have been postulated to be involved in a variety of signaling processes, ranging from a relatively well-established role in neuromodulation,[3] insulin secretion,[4,5] and fertilization[6,7] to its proposed role as a secondary messenger in intracellular signaling.[8,9] The high intrinsic affinity of Zn^{2+} for the amino acid side chains of cysteines, histidines, as well as carboxylic acids makes the free Zn^{2+} ion a potent inhibitor of enzymes and a potential modulator of protein−protein interactions.[10−12] The level of free Zn^{2+} in the cytosol is therefore believed to be tightly controlled between 100 pM and 1 nM,[13−15] which is sufficient for Zn^{2+} to bind to native Zn-binding proteins but low enough not to interfere with normal metabolic and signaling processes.[16] The concentration of free Zn^{2+} can be very different in other parts of the cell, however, as millimolar concentrations of total Zn^{2+} have been reported for secretory vesicles in pancreatic β cells,[17] oocytes,[7] neuronal cells,[18] and mast cells.[19] Triggered release of Zn^{2+} from organelles has been implicated in transient increases in cytosolic free Zn^{2+}, potentially regulating the activity of regulatory enzymes such as protein phosphatases and caspases.[8,9]

To get a better understanding of intracellular Zn^{2+} homeostasis and the putative signaling role of Zn^{2+}, a variety of fluorescent sensors have been developed that allow monitoring of Zn^{2+} concentrations in single living cells in real time. Although small molecule sensors are still the most commonly used imaging probes,[20,21] it has proven challenging to control their subcellular localization and concentration. In contrast, genetically encoded, protein-based sensors can be conveniently targeted to specific subcellular locations and, at least in the cytosol, were found to not perturb intracellular free Zn^{2+} levels.[13,22,23] Thus far, two families of genetically encoded FRET-based Zn^{2+} sensors have been most widely applied: the eCALWY[13] sensors developed by our group and the ZapCY

Received: March 24, 2015
Accepted: July 7, 2015

DOI: 10.1021/acschembio.5b00211
ACS Chem. Biol. XXXX, XXX, XXX−XXX

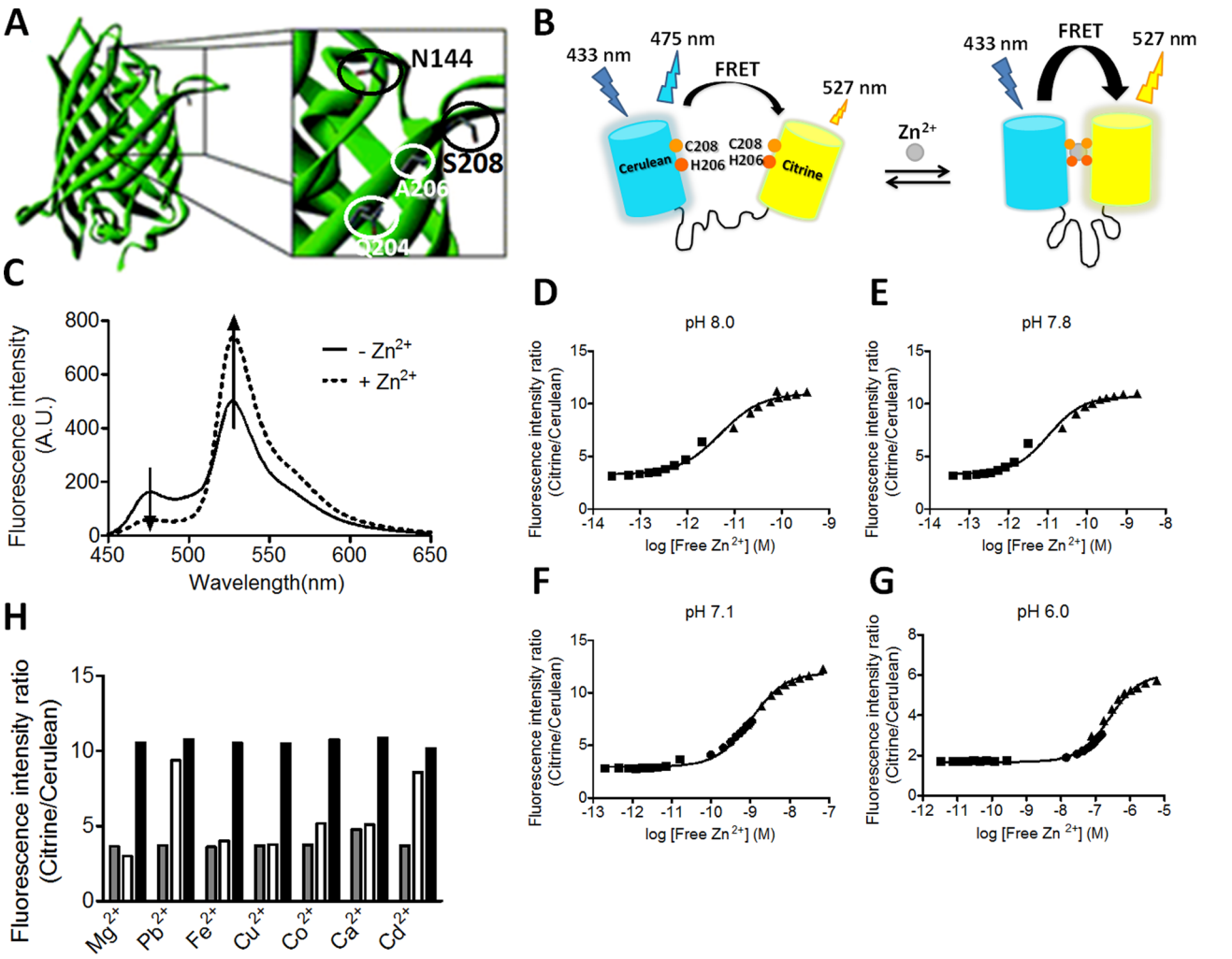

Figure 1. Design and Zn^{2+} binding properties of eZinCh-2. (A) Crystal structure of green fluorescent protein (PDB code: 1GFL)[33] showing the positions that were used to introduce cysteine or histidine residues. (B) eZinCh-2 sensor design containing a Cys_2His_2 binding pocket on the dimerization interface of both fluorescent proteins. (C) Emission spectra of eZinCh-2 before (empty) and after (Zn^{2+} saturated) addtion of Zn^{2+}. (D–G) Zn^{2+} titrations of eZinCh-2 at different pH's, showing the emission ratio of citrine over cerulean as a function of Zn^{2+} concentration. To obtain picomolar to micromolar free Zn^{2+} concentrations, HEDTA (squares) and different amounts of EGTA (5 mM and 1 mM, circles and triangles, respectively) were used as buffering systems (Tables S2–S5). Solid lines represent a fit assuming a 1:1 binding event, yielding K_d's of 256 nM (pH 6.0), 1.03 nM (pH 7.1), 10 pM (pH 7.8), and 5 pM (pH 8.0). Measurements were performed in 150 mM MES (pH 6.0), 150 mM HEPES (pH 7.1), or 50 mM Tris (pH 7.8 and 8.0) and 100 mM NaCl, 10% (v/v) glycerol, 0.01% Tween and 1 mM DTT at 20 °C. (H) Emission ratio of eZinCh-2 before (gray bars) and after (white bars) the addition of Pb^{2+}, Fe^{2+}, Cu^{2+}, Co^{2+}, or Cd^{2+} (all 20 μM) or Mg^{2+} or Ca^{2+} (both 0.5 mM) in the presence of 10 μM TPEN. The black bars show the emission ratio upon subsequent addition of 20 μM Zn^{2+}.

sensors developed by Palmer and co-workers.[14] These FRET-based sensors are ratiometric and display at least a 2-fold change in emission ratio upon binding Zn^{2+} at physiological pH. Their affinities have been tuned within the picomolar to nanomolar range, and for both families red-shifted variants have been developed to allow multiparameter imaging.[24,25] The eCALWY sensors consist of two small, CXXC-motif-containing metal binding domains (ATOX1 and WD4), connected by a long and flexible peptide linker, which in turn are linked to self-associating variants of cerulean and citrine. Formation of a tetrahedral Zn^{2+} complex between the metal binding domains disrupts the interaction between the fluorescent domains, resulting in a decrease in citrine/cerulean emission ratio. Substitution of one of the cysteines by a serine in the WD4 domain decreased the Zn^{2+} affinity from 2 pM in eCALWY-1 to 630 pM in eCALWY-4, whereas shortening of the linker between the metal binding domains allowed more subtle attenuation of the Zn^{2+} affinity. Application of these eCALWY sensors for measuring concentrations of cytosolic Zn^{2+} in various cell types and organisms has shown that cytosolic Zn^{2+} concentrations are typically between 100 pM and 1 nM, rendering the eCALWY-4 variant the sensor of choice for cytosolic Zn^{2+} imaging. The ZapCY family of sensors contains the first two zinc finger domains from the Zn^{2+}-responsive transcriptional regulator Zap1. ZapCY1, the sensor containing the wild-type zinc finger domains, displayed an increase in FRET following Zn^{2+}-induced folding of the zinc finger domains with a K_d of 2.5 pM.[14] Consistent with the results obtained with the eCALWY sensors, this sensor was found to be fully saturated with Zn^{2+} when expressed in the cytosol of HeLa cells. Therefore, a lower affinity variant has been constructed by replacing two of the Zn^{2+} coordinating residues by histidines, yielding a sensor with a K_d of 811 pM.[14]

DOI: 10.1021/acschembio.5b00211
ACS Chem. Biol. XXXX, XXX, XXX–XXX

Both the eCALWY and ZapCY sensors have been successfully applied to measure cytosolic free Zn^{2+} in a number of different cell types (primary cells, cell lines) originating from various organisms (bacterial, yeast, mammalian, and plant cells).[15,22,26−28] However, while both sensors report similar values for free Zn^{2+} when expressed in the cytosol, they respond differently when targeted to other organelles such as the ER and the mitochondria.[15,28,29] ZapCY1 targeted to the ER and mitochondria was found to be mostly Zn^{2+}-free, which, because of the high affinity ZapCY1, would be consistent with very low concentrations of free Zn^{2+} of 0.9 pM and 0.22 pM in the ER and mitochondria, respectively. More recent studies using the eCALWY sensors reported free Zn^{2+} concentrations in the ER and mitochondria that are 2−3 orders of magnitude higher, however.[15] The reason for this strikingly different behavior is unclear, but one way to resolve this discrepancy is to develop alternative FRET sensors based on a different binding mechanism. Another incentive for the development of alternative FRET sensors is a need for probes with affinities that are tuned to specific applications, such as measuring the relatively high free Zn^{2+} concentrations under the acidic conditions present in secretory vesicles.

We previously reported the construction of an alternative FRET sensor that lacked separate metal binding domains, but in which Zn^{2+}-coordinating amino acids were introduced directly at the so-called dimerization interface of two fluorescent domains.[30] The first generation of these ZinCh sensors showed a large ratiometric change upon Zn^{2+} binding, but the Zn^{2+} affinity was relatively low (K_d = 8.2 μM at pH 7.1).[13] Here, we show that combining histidine and cysteine coordination to create a Cys_2His_2 binding pocket on the dimerization interface can increase the affinity for Zn^{2+} over 1000-fold. This new sensor variant, eZinCh-2, has an affinity that is similar to that of eCALWY-4 (K_d = 1 nM at pH 7.1),[13] but a substantially larger change in emission ratio. eZinCh-2 not only provides an attractive alternative for measuring Zn^{2+} in the cytosol but was also successfully used for measuring Zn^{2+} in the ER, mitochondria, and even dense core secretory vesicles, providing an independent system for assessing the free Zn^{2+} concentrations in these organelles. Moreover, organelle-targeted eZinCh-2 provides an attractive sensor to be used in combination with our previously reported red eCALWY variants to allow multicolor imaging of intracellular Zn^{2+} simultaneously in the cytosol and the ER or mitochondria.

RESULTS AND DISCUSSION

Development and *in Vitro* Characterization of eZinCh-2. In an effort to create high affinity Zn^{2+} binding sites at the dimerization interface of the eZinCh FRET sensor, we previously created several variants with two cysteines on each of the two fluorescent domains (C144/C206, C206/C208, and C206/C204; Figure 1A).[31] None of these variants showed enhanced affinity for Zn^{2+} compared to the parent sensor eZinCh-1, which contained a single Cys at position 208. Increased affinity was observed for Cd^{2+}, a metal ion with similar coordination properties as Zn^{2+}, but a larger ionic radius.[31] Modeling showed that the Cys_4 binding pocket created by displaying cysteines on a β-barrel scaffold in these variants was too large to allow simultaneous coordination of Zn^{2+} by all four cysteines and suggested that a binding site consisting of a combination of cysteines and histidines might provide a better Zn^{2+} binding site.[32] We therefore screened a small collection of sensor variants in which one or two of the cysteines were mutated to histidines for increased Zn^{2+} affinity at pH 7.1. Three variants were found with a Zn^{2+} affinity in the low nanomolar range at pH 7.1 (Supporting Table 1; Supporting Figure 1), which is 3 orders of magnitude higher compared to the original eZinCh sensors. Only one sensor displayed a large, 4-fold change in emission ratio, whereas the other two showed ∼10% changes in emission ratio. This sensor variant, which contains a cysteine at position 208 and a histidine at position 206 on both domains, was further characterized *in vitro* and will be referred to as eZinCh-2 (Figure 1). The small change in emission ratio observed for the other two variants could be due to an unfavorable orientation of the two fluorescent domains in the Zn^{2+}-bound state, resulting in a low value for the orientation factor κ and relative inefficient energy transfer.

Zn^{2+} titration experiments were done to determine the Zn^{2+} affinity of eZinch-2 at different, physiologically relevant pH's. At pH 7.1, which is the pH of the cytosol and the ER lumen, eZinCh-2 binds Zn^{2+} with a K_d of 1.0 ± 0.1 nM. This affinity is similar to that of eCALWY-4 at this pH, whereas the change in emission ratio for eZinCh-2 is 2-fold higher (400% vs 200%). Titrations done at pH 6, the pH representative of vesicular conditions, yielded a K_d of 256 ± 22 nM. This affinity is still 3 orders of magnitude higher than that of its predecessor eZinCh-1, while retaining a large, 300% change in emission ratio. As expected, increasing the pH results in stronger Zn^{2+} binding, yielding K_d values of 5 and 10 pM at pH 8 and 7.8, respectively. The affinity of eZinCh-2 at pH 7.8, which is representative of the pH in the mitochondrial matrix, is 6-fold stronger than that of eCALWY-4. Based on these Zn^{2+} affinities, the eZinCh-2 sensor may represent a versatile sensor to measure Zn^{2+} not only in the cytosol but also in the ER, mitochondrial matrix, and secretory vesicles. However, since the Cys_2His_2 site at the dimerization interface in eZinCh-2 was created *de novo*, it was important to first assess its metal specificity. The emission ratio of eZinCh-2 was therefore measured in the presence of a wide variety of metal ions (20 μM or 5 mM) and 10 μM of the zinc chelator TPEN (Figure 1G). An increase in emission ratio was observed for Cd^{2+} and Pb^{2+}, which was not unexpected as these metal ions have similar coordination properties to Zn^{2+}. However, no significant changes were observed for physiological relevant metal ions such as Fe^{2+}, Cu^{2+}, Mg^{2+}, or Ca^{2+}. To test whether these metal ions might still compete with Zn^{2+} binding and in this way interfere with Zn^{2+} sensing, the emission ratio was also determined upon subsequent addition of 20 μM Zn^{2+}. None of the metals had any effect on the Zn^{2+} binding response, however.

Using eZinCh-2 to Monitor Intracellular Free Zn^{2+} Concentrations in the Cytosol. Its Zn^{2+} affinity of 1 nM at pH 7.1, together with its 4-fold change in emission ratio, makes eZinCh-2 an attractive alternative to eCALWY-4 and ZapCY2 for measuring cytosolic free Zn^{2+} levels. The eZinCh-2 construct was cloned into a plasmid containing a CMV promoter for transient expression, and the performance of eZinCh-2 was tested in four different mammalian cell lines. HeLa and HEK293T cells were chosen because these cells were previously used for the *in situ* characterization of the eCALWY and ZapCY sensors.[13,28] In addition, we also used eZinCh-2 to determine the cytosolic free Zn^{2+} concentration in wild-type (MCF-7) and tamoxifen-resistant MCF-7 (TamR) breast cancer cell lines. These breast cancer cell lines were chosen because previous work using small molecule fluorescent sensors reported increased levels of intracellular Zn^{2+} in TamR cells

DOI: 10.1021/acschembio.5b00211
ACS Chem. Biol. XXXX, XXX, XXX−XXX

compared to wild-type MCF-7 cells.[34,35] The performance of eZinCh-2 was assessed by monitoring the response of the eZinCh-2 sensor in single living cells to the subsequent addition of the strong membrane-permeable Zn^{2+} chelator TPEN, followed by the addition of excess Zn^{2+} together with the Zn^{2+} specific ionophore pyrithione (Figure 2). In all cell lines tested, a robust, 3-fold change in citrine over cerulean emission ratio was observed between the Zn^{2+}-depleted and Zn^{2+}-saturated states of the sensor. eZinCh-2 also showed relatively fast *in situ* association and dissociation kinetics, and low variability between individual cells. The determination of R_{min} and R_{max} allowed calculation of the sensor occupancy at the start of the experiment, which could be translated into a free Zn^{2+} concentration using the K_d of 1 nM that was measured *in vitro*. Very similar free Zn^{2+} concentrations of 0.87 ± 0.10 nM and 0.83 ± 0.10 nM were determined for HeLa and HEK293 cells, respectively. These numbers agree reasonably well with values determined previously using the eCALWY and ZapCY sensors in the same cell types. Slightly lower concentrations of free Zn^{2+} were measured in wild type MCF-7 cells (0.44 ± 0.06 nM) and TamR cells (0.65 ± 0.06 nM). These results show that cytosolic Zn^{2+} concentrations are well-buffered and relatively constant among different mammalian cell types, in particular when one considers that cell lines were grown under slightly different conditions, each optimal for that specific cell type. In addition, the increased levels of intracellular Zn^{2+} that were previously reported for TamR cells, apparently do not translate into a large increase in the concentration of free Zn^{2+} in the cytosol of these cells.

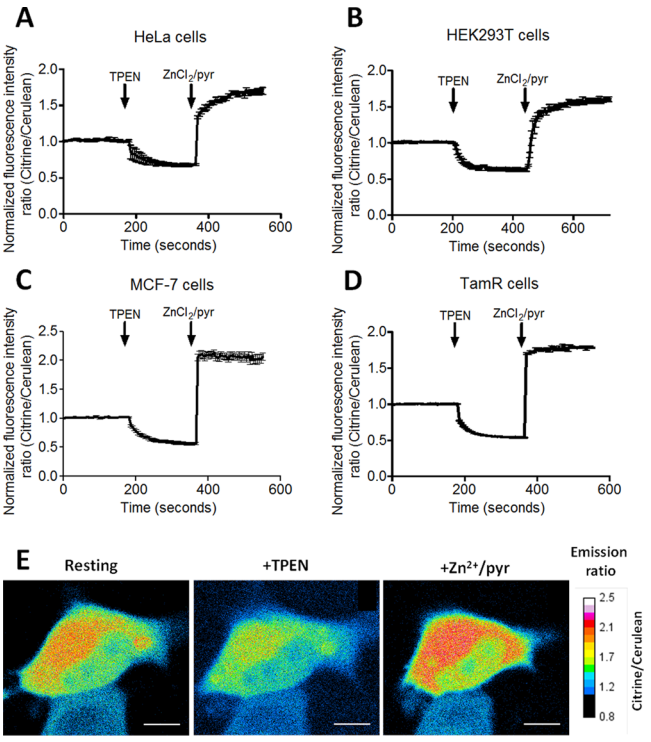

Figure 2. Determination of the free cytosolic Zn^{2+} concentration in different cell types using eZinCh-2. (A–D) Responses of HeLa (A), HEK293T (B), MCF-7 (C), and TamR (D) cells expressing eZinCh-2 to the addition of 50 μM TPEN, followed by the addition of 100 μM Zn^{2+}/ 5 μM pyrithione. All traces in A–D represent the average of at least four cells after normalization of the emission ratio at $t = 0$. Error bars represent SEM. (E) False colored ratiometric images of a HeLa cell expressing eZinCh-2 in a resting state (start), after perfusion with 50 μM TPEN (+TPEN), and 100 μM $ZnCl_2$/5 μM pyrithione (+Zn/pyr).

Targeting of eZinCh-2 to the Endoplasmic Reticulum. Following the robust performance of eZinCh-2 in imaging cytosolic Zn^{2+}, we next explored its suitability for measuring free Zn^{2+} in the ER. eZinCh-2 was targeted to the lumen of the ER by introducing a preproinsulin (PPI) signal peptide sequence at the N-terminus and a C-terminal retention sequence KDEL, yielding ER-eZinCh-2. Co-staining with a commercially available ER tracker (ER-tracker Red, Life Technologies) confirmed correct targeting of ER-eZinCh-2 in HeLa cells (Figure 3A). The addition of TPEN to HeLa cells expressing ER-eZinCh-2 showed a decrease in emission ratio that was stable after a few minutes. Subsequent addition of excess Zn^{2+} in the presence of pyrithione resulted in an immediate increase in emission ratio. Based on these traces, a free Zn^{2+} concentration of 0.8 ± 0.6 nM was determined for the ER in HeLa cells. The large standard error for the estimated Zn^{2+} levels reflects relatively high cell-to-cell variability, with some cells showing a concentration of 1.5 nM, while others contain only 0.3 nM. Although these concentrations are slightly lower than estimated using ER-targeted eCALWY-4,[15] these values are still at least 100-fold higher than the concentration estimated using ZapCY1 in HeLa cells.[28]

Previous work by Taylor and co-workers showed increased expression of ZIP7 in TamR cells compared to wild type MCF-7 cells. ZIP7 is a Zn^{2+} transporter protein located almost exclusively on the ER membrane. Phosphorylation of ZIP7 was shown to activate the importer, resulting in release of Zn^{2+} from the ER into the cytosol.[9] To establish whether TamR cells have increased concentrations of free Zn^{2+} in the ER, ER-ZinCh-2 was expressed in both wild-type MCF-7 and TamR cells (Figure 3C,D). The addition of TPEN and excess Zn^{2+} showed similar response curves to those found in HeLa cells, yielding free ER Zn^{2+} concentrations of 0.54 ± 0.27 nM for MCF-7 and 0.75 ± 0.49 nM for TamR cells. Please note that R_{max} was determined using the immediate, rapid increase in emission ratio following the addition of excess Zn^{2+}. Control measurements using ER-targeted eCALWY-4 gave similar ER Zn^{2+} concentrations of 0.39 ± 0.17 nM and 0.21 ± 0.05 nM for MCF-7 and TamR cells, respectively (Supporting Figure 2). Again, the cell-to-cell variation in free Zn^{2+} concentration was found to be larger in the ER when compared to the cytosol, which may reflect more efficient buffering of the free Zn^{2+} concentration in the cytosol due to the presence of metallothionein.

Targeting eZinCh-2 to Mitochondria and Insulin-Secreting Vesicles. To explore whether eZinCh-2 could also be successfully applied to other organelles, we targeted the sensor to the mitochondrial matrix in HeLa cells and to insulin-secreting vesicles in INS-1 (832/13) cells, a rat pancreatic beta cell line. Targeting to the mitochondrial matrix was achieved by introducing the N-terminal targeting sequence from cytochrome *c* oxidase subunit VIII (Cox VIII), yielding mito-eZinCh-2. Co-staining HeLa cells expressing mito-eZinCh-2 with MitoTracker Red (Life Technologies) confirmed correct targeting of the genetically encoded Zn^{2+} probe to this compartment (Figure 4A). A robust response to the addition of TPEN and excess Zn^{2+} was observed (Figure 4B), showing an average occupancy of the sensor of 23 ± 6% (Figure 4B). Assuming an intramitochondrial pH of 7.8, and thus a K_d of 10 pM for eZinCh-2, this number translates into a mitochondrial

DOI: 10.1021/acschembio.5b00211
ACS Chem. Biol. XXXX, XXX, XXX–XXX

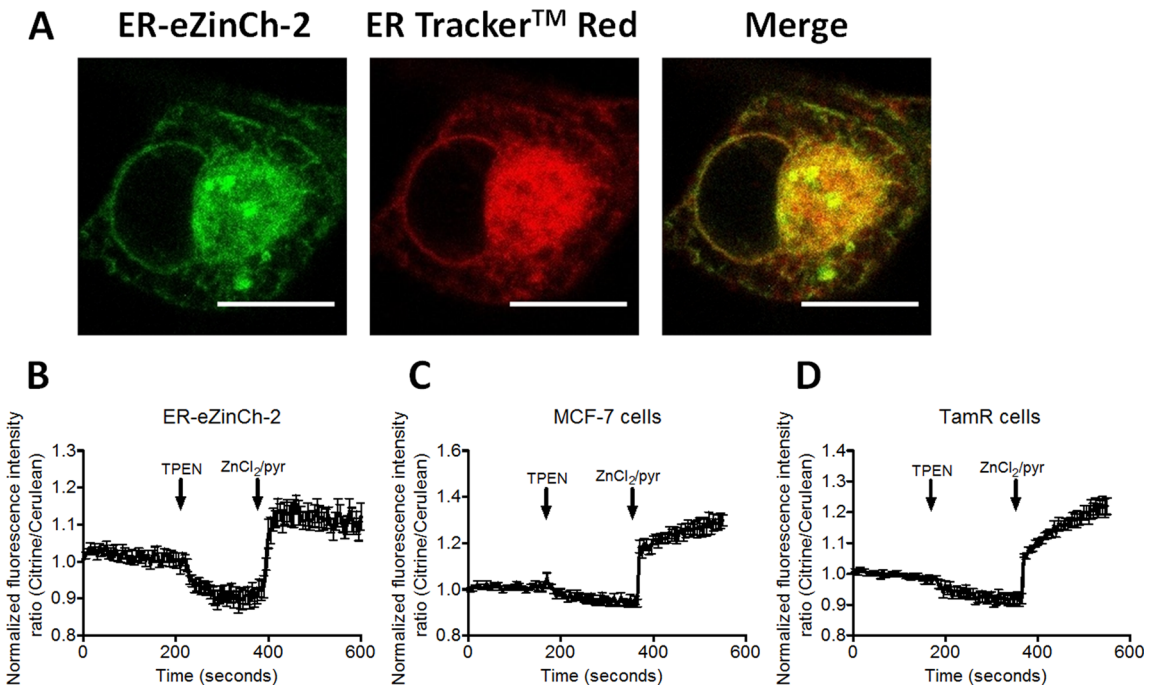

Figure 3. Zn^{2+} imaging using ER-targeted eZinCh-2 in different cells types. (A) Fluorescent confocal images of a HeLa cell expressing ER-eZinCh-2 in the endoplasmic reticulum, costained with ER-tracker red. Pearson's coefficient, 0.936. Scale bar, 15 μm. (B–D) Responses of HeLa (B), MCF-7 (C), and TamR (D) cells expressing ER-eZinCh-2 to the addition of 50 μM TPEN, followed by the addition of 100 μM Zn^{2+}/5 μM pyrithione. All traces in B–D represent the average of at least four cells after normalization of the emission ratio at t = 0. Error bars represent SEM.

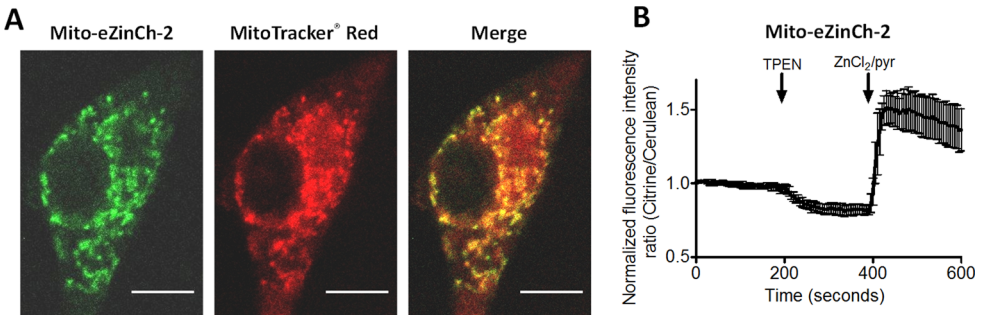

Figure 4. Targeting of eZinCh-2 to the mitochondrial matrix. (A) Fluorescent confocal images of a HeLa cell expressing the mitochondrial targeted mito-eZinCh-2, costained with MitoTracker Red. Pearson's coefficient, 0.895. Scale bar, 10 μm. (B) Response of mito-eZinCh-2 expressed in HeLa cells upon the addition of 50 μM TPEN, followed by the addition of excess 100 μM Zn^{2+}/5 μM pyrithione. The trace in B represent the average of four cells after normalization of the emission ratio at t = 0. Error bars represent SEM.

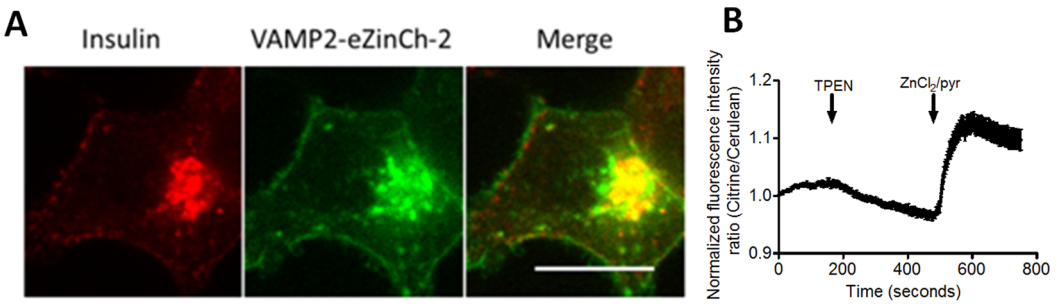

Figure 5. Targeting of eZinCh-2 to insulin secreting vesicles. (A) Overlay of the fluorescent confocal images of INS-1 (832/13) cells expressing vesicular targeted VAMP2-eZinCh-2, costained for insulin. Pearson's coefficient, 0.83. Scale bar, 15 μm. (C) Ratiometric response of INS-1 (832/13) cells expressing VAMP2-eZinCh-2 to perfusion with 50 μM TPEN, or 100 μM Zn^{2+}/5 μM pyrithione. Traces in C represent the average of 10 cells after normalization of the emission ratio at t = 0. Error bars represent SEM.

matrix Zn^{2+} concentration of 3.3 ± 1.2 pM. Experiments under identical conditions in the same cells using mito-eCALWY-4 yielded a somewhat higher concentration of about 42 ± 28 pM (Supporting Figure 3; Table S6). These mitochondrial free Zn^{2+} concentrations are in between those previously reported using eCALWY-4 (~200 pM) in a number of cell lines and the

DOI: 10.1021/acschembio.5b00211
ACS Chem. Biol. XXXX, XXX, XXX–XXX

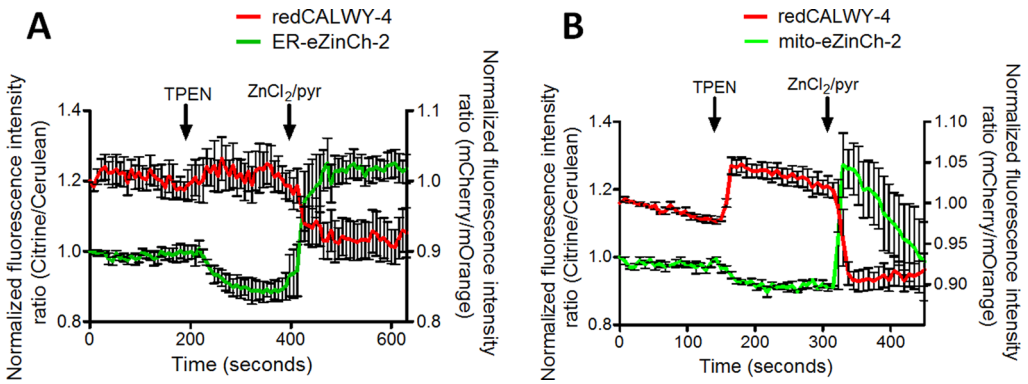

Figure 6. Responses of HeLa cells expressing both redCALWY-4 (red) and either ER-eZinCh-2 (A) or mito-eZinCh-2 (B) (green) to the addition of 50 μM TPEN, followed by the addition of excess 100 μM Zn^{2+}/5 μM pyrithione. Traces in A and B represent the average of at least four cells after normalization of the emission ratio at t = 0. Error bars represent SEM.

0.14 pM determined using the ZapCY-1 sensors.[29] A value of 0.2 pM has also been reported by Thompson and co-workers using a carbonic anhydrase based FRET sensor,[36] while a concentration of 72 pM has been determined using a small molecule ratiometric fluorescent probe targeted to the mitochondria of NIH3T3 cells.[37] Because the Zn^{2+} affinities of both eZinCh-2 and the other two FRET sensors are strongly pH sensitive, it is important to note that these values will be very dependent on the exact pH of the mitochondrial matrix, however.

In an effort to determine the free Zn^{2+} concentrations in secretory vesicles, we previously targeted both the eCALWY sensors and the eZinCh-1 sensor to insulin granules of INS-1 (832/13) cells by fusing them to the vesicle-targeted membrane protein 2 (VAMP2). However, neither of these sensors showed changes in emission ratio upon the addition of TPEN or Zn^{2+}/pyrithione. Vesicular targeting of eZinCh-2 was performed similarly by fusion of VAMP-2 to the N-terminus of eZinCh-2. Co-staining of VAMP2-eZinCh-2 with an insulin-specific antibody revealed significant localization to insulin-containing granules as expected (Figure 5A).

Interestingly, vesicular-targeted eZinCh-2 was found to be responsive to the addition of TPEN and Zn^{2+}/pyrithione (Figure 5B). A relatively slow decrease in emission ratio was observed upon the addition of TPEN, suggesting that prolonged incubation with TPEN is required to lower the relatively high free Zn^{2+} concentration in these vesicles. Subsequent addition of Zn^{2+}/pyrithione induced a relatively rapid increase in emission ratio. Although it is more difficult to determine the sensor occupancy very accurately in this case, VAMP2-eZinCh-2 appeared to be ~30% saturated, which, assuming an intragranular pH of 6,[38] corresponds to a free Zn^{2+} concentration of ~120 nM. Also in this case, more accurate determination of these values will require independent assessment of the vesicular pH. Nonetheless, as far as we know, these results represent the first successful application of a genetically encoded fluorescent sensor for vesicular Zn^{2+}.

Multicolor Imaging. The results shown above prove that eZinCh-2 is a versatile Zn^{2+} sensor that can be applied to monitor the free Zn^{2+} concentrations in a number of different organelles. eZinCh-2 would therefore be an attractive sensor to use in conjunction with one of the recently developed red-shifted cytosolic eCALWY sensors to allow simultaneous monitoring of cytosolic and organelle Zn^{2+} concentrations in a single cell. To explore the feasibility of using eZinCh-2 for multicolor imaging, we coexpressed the cytosolic redCALWY-4 sensor with either ER-ZinCh-2 or mito-eZinCh-2 in HeLa cells. redCALWY-4 is a red-shifted variant of eCALWY-4 in which the original cerulean and citrine fluorescent domains have been replaced by self-associating variants of the mOrange2 and mCherry, respectively.[24] Figure 6A shows that coexpression of cytosolic redCALWY-4 together with ER-eZinCh-2 allows simultaneous monitoring of Zn^{2+} levels in both the ER and the cytosol (Figure 6A). The response of each sensor to the addition of TPEN or excess Zn^{2+} was similar to what was observed in single sensor measurements. The addition of TPEN resulted in an increase in acceptor/donor emission ratio for redCALWY-4 and a decrease in acceptor/donor emission ratio for ER-eZinCh-2, both consistent with a simultaneous decrease in cytosolic and ER Zn^{2+} levels. The opposite behavior was observed upon the addition of excess Zn^{2+}/pyrithione. Successful multicolor imaging was also achieved when coexpressing redCAWY-4 with mito-eZinCh-2. Again, multicolor imaging allowed independent monitoring of both cytosolic and mitochondrial free Zn^{2+} in the same cell, with each sensor behaving as expected based on single sensor experiments. Because of their smaller volume, imaging in organelles is typically more challenging than measuring in the cytosol. In this case, the organelle Zn^{2+} status was more easily measured than the cytosolic Zn^{2+} concentration, however. This is partly due to the relatively low expression levels of the redCALWY sensors, but also a testament of the robust nature of the organelle-targeted eZinCh-2 sensors.

Conclusion. A *de novo* metal binding site with a remarkable high affinity for Zn^{2+} was created on the dimerization interface of two fluorescent domains by using a combination of cysteine and histidine coordination. The development of the eZinCh-2 sensor did not require extensive evolution or precise tuning of the secondary coordination sphere, suggesting that a similar strategy could be applied to construct FRET sensors based on different fluorescent proteins (e.g., mOrange/mCherry) or introduce Zn^{2+}-dependent control of other protein−protein interactions. Although the high affinity is consistent with the formation of a Cys_2His_2 complex, definite proof for such coordination should come from X-ray structure determination and/or EXAFS. This could also help to further optimize the Zn^{2+} affinity. Alternatively, directed evolution could be envisioned to identify variants of eZinCh-2 with even higher affinity or larger change in emission ratio.

eZinCh-2 provides an attractive alternative to the previously developed FRET sensors of the eCALWY and ZapCY series (Table S6). The lack of separate metal binding domains makes

DOI: 10.1021/acschembio.5b00211
ACS Chem. Biol. XXXX, XXX, XXX−XXX

the sensor architecture of eZinCh-2 relatively simple, which may explain the robust expression of eZinCh-2 in all the cell lines we tested. The unique binding mechanism not only ensures a large difference in FRET between the on and off state of the sensor but also provides an opportunity to help resolve some of the contradictory results obtained with the eCALWY and ZapCY sensors. Although the free Zn^{2+} concentration in the ER was found to be more heterogeneous than in the cytosol, the results obtained with ER-targeted eZinCh-2 largely confirmed previous experiments using ER-targeted eCALWY-4[15] and are inconsistent with the very low, sub-picomolar concentrations of free Zn^{2+} determined using ZapCY1.[28] When targeted to the mitochondrial matrix eZinCh-2 reported Zn^{2+} concentrations that are between those reported by the eCALWY-4 probe and the ZapCY1 probe. More definite determination of the mitochondrial free Zn^{2+} concentration should ideally also involve the experimental determination of the mitochondrial pH, as the Zn^{2+} affinities of these sensors are known to be strongly pH dependent in this regime. The same strategy is also recommended for future applications in which eZinCh-2 is used to measure vesicular Zn^{2+}.

METHODS

Cloning Strategies and Protein Expression and Purification. A detailed description of cloning strategies to create several eZinCh mutants and ER and mitochondrial targeted eZinCh-2 probes, as well as protein expression and purification strategies, can be found in the Supporting Information.

Zn^{2+} Titration Experiments. Zn^{2+} titrations were carried out with 1 μM of different eZinCh variants in 2 mL of buffer consisting of 150 mM MES (pH 6.0), 150 mM HEPES (pH 7.1) or 50 mM Tris (pH 7.8 and 8.0), 100 mM NaCl, 10% (v/v) glycerol, 0.01% Tween, and 1 mM DTT at 20 °C.[30] Different Zn^{2+}-chelators (HEDTA and EGTA) were used together with increasing Zn^{2+} concentrations to reach the desired free Zn^{2+} concentration. These free Zn^{2+} concentrations were calculated using the MaxChelator program (http://maxchelator.stanford.edu/). To determine the dissociation constants (K_d) for Zn^{2+} of eZinCh-2 at different pH's, the emission ratio was fitted as a function of $[Zn^{2+}]$ using eq 1.

$$R = \frac{P_1 \cdot [Zn^{2+}]}{K_d + [Zn^{2+}]} + P_2 \quad (1)$$

In eq 1, R is the ratio of citrine (at 527 nm) to cerulean (at 475 nm) emission, $[Zn^{2+}]$ is the calculated free Zn^{2+} concentration in M, P_1 is defined as the ratiometric change upon Zn^{2+} binding, P_2 is the ratio (Cit/Cer) in the absence of Zn^{2+}, and K_d is the dissociation constant in M.

Mammalian Cell Culture and Imaging. HeLa cells were cultured in Dulbecco's Modified Eagle Medium (DMEM) supplemented with 25 mM glucose, 10% (v/v) fetal bovine serum (FBS), 2 mM glutamine, 100 U/mL penicillin, and 100 μg/mL streptomycin in a humidified atmosphere containing 5% CO_2. MCF-7 and TamR cells were cultured in Roswell Park Memorial Institute media (RPMI), supplemented with 5% (v/v) fetal calf serum (FCS), 2 mM glutamine, 1 mM fungizone, 100 U/mL penicillin, and 100 μg/mL streptomycin at the same temperature and CO_2 levels; for TamR cells, the media were supplemented with 10^{-7} M 4-hydroxytamoxifen. For TamR cells, developed as described previously,[39] stripped fetal calf serum (SFCS) was used instead of FBS. INS-1 (832/13) cells were cultured at 37 °C/5% CO_2 in RPMI-1640 medium containing 10% (v/v) FBS, 10 mM HEPES, 2 mM glutamine, 1 mM sodium-pyruvate, 50 μM β-mercaptoethanol, 100 U/mL penicillin, and 100 μg/mL streptomycin (all from Life Technologies). Cells were seeded on glass coverslips (ø 30 mm, VWR) 1 day before transfection. About 200 000 cells were seeded to reach a confluency of ~80% on the day of transfection. Lipofectamine 2000 (Life Technologies) was used to carry out transfections, following the manufacturer's instructions. Cells were imaged either 1 day (single sensor experiments) or 2 days (two sensor experiments) after transfection in a HEPES buffer (Live Cell Imaging Buffer, Life Technologies) at 37 °C. Imaging on Hek293T, HeLa, MCF-7, and TamR cells was performed with a confocal microscope (Leica, TCS SP5X) equipped with a 63× water immersion objective, acousto-optical beamsplitters (AOBS), a white light laser, and a 405 nm laser. A black box was installed around the stage of the microscope to avoid surrounding light coming in, and the temperature inside this box was controlled at 37 °C using a temperature controller. For all CFP-YFP based constructs, except for the vesicular targeted sensor, cerulean was excited using the 405 nm laser. For the redCALWY-4, the white light laser was set to 550 nm (5% of full power) to excite mOrange2. Emission was monitored using the AOBS and avalanche photo diode/photomultiplier tubes hybrid detectors (HyD, Leica): cerulean (450−500), citrine (515−595 nm), mOrange2 (565−600), and mCherry (600−630). Images were recorded at either 7.5 s intervals (two sensor experiments) or at 5 s intervals (single sensor experiments). Secretory granule free Zn^{2+} was imaged in INS1(832/13) cells expressing VAMP2-eZinCh-2 using the protocol described in ref 15 using an Olympus IX-70 wide-field microscope with a 40x/1.35NA oil immersion objective and a zyla sCMOS camera (Andor Technology, Belfast, UK) controlled by Micromanager software.[40] Excitation was provided at 433 nm using a monochromator (Polychrome IV, Till Photonics, Munich, Germany). Emitted light was split and filtered with a Dual-View beam splitter (Photometrics, Tucson, AZ, USA) equipped with a 505dcxn dichroic mirror and two emission filters (Chroma Technology, Bellows Falls, VT, USA - D470/24 for cerulean and D535/30 for citrine). Images were acquired at 3 s intervals

Cells were perfused for a few minutes with HEPES buffer without additives; next the buffer was changed to a HEPES buffer containing 50 μM N,N,N′,N′-tetrakis(2-pyridylmethyl)ethylenediamine (TPEN, Sigma) for a few minutes, followed by perfusion with HEPES buffer containing 100 μM $ZnCl_2$ and 5 μM of the Zn^{2+}-specific ionophore 2-mercaptopyridine N-oxide (pyrithione, Sigma). Imaging experiments on INS1(832/13) cells were performed using KREBS buffer.[13] All buffers were kept at 37 °C during imaging using a water bath.

Image analysis was performed using ImageJ software as described before.[15,41] The steady-state fluorescence intensity ratio of acceptor over donor was measured, followed by the determination of the minimum and maximum ratios to calculate the free Zn^{2+} concentration using the following formula:

$$[Zn^{2+}] = K_d \cdot (R - R_{min})/(R_{max} - R)$$

in which R_{min} is the ratio in the Zn^{2+} depleted state, after the addition of 50 μM TPEN, and R_{max} was obtained upon Zn^{2+} saturation with 100 μM $ZnCl_2$ in the presence of 5 μM pyrithione.

ASSOCIATED CONTENT

Supporting Information

Molecular cloning methods, protein purification methods, primer sequences. Additional titration data, ER-eZinCh-2 MCF-7 and TamR cell measurements, Mito-eZinCh-2 HeLa cell measurements, and nucleotide sequences for expression constructs. The Supporting Information is available free of charge on the ACS Publications website at DOI: 10.1021/acschembio.5b00211.

AUTHOR INFORMATION

Corresponding Author

*Tel.: +31(0)402474728. E-mail: m.merkx@tue.nl.

Notes

The authors declare no competing financial interest.

DOI: 10.1021/acschembio.5b00211
ACS Chem. Biol. XXXX, XXX, XXX−XXX

■ ACKNOWLEDGMENTS

The work of A.M.H. and M.M. was supported by an ECHO grant from The Netherlands Organization of Scientific Research (700.59.013) and an ERC starting grant (ERC-2011-StG 280255). This work was supported by an STSM Grant from COST Action TD1304 (ZincNet). G.A.R. was funded by a Wellcome Trust Senior Investigator Award (WT098424AIA) and a Royal Society Wolfson Research Merit Award. K.M.T. acknowledges the support of a Wellcome Trust University award (091991/Z/10/Z), and we thank Julia Gee for the use of the TAMR cells.

■ REFERENCES

(1) Vallee, B. L., and Falchuk, K. H. (1993) The biochemical basis of zinc physiology. *Physiol. Rev. 73*, 79−118.
(2) Maret, W. (2009) Molecular aspects of human cellular zinc homeostasis: redox control of zinc potentials and zinc signals. *BioMetals 22*, 149−157.
(3) Frederickson, C. J., Koh, J. Y., and Bush, A. I. (2005) The neurobiology of zinc in health and disease. *Nat. Rev. Neurosci. 6*, 449−462.
(4) Li, D., Chen, S., Bellomo, E. A., Tarasov, A. I., Kaut, C., Rutter, G. A., and Li, W. H. (2011) Imaging dynamic insulin release using a fluorescent zinc indicator for monitoring induced exocytotic release (ZIMIR). *Proc. Natl. Acad. Sci. U. S. A. 108*, 21063−21068.
(5) Li, D., Liu, L., and Li, W. H. (2015) Genetic targeting of a small fluorescent zinc indicator to cell surface for monitoring zinc secretion. *ACS Chem. Biol. 10*, 1054−1063.
(6) Kim, A. M., Bernhardt, M. L., Kong, B. Y., Ahn, R. W., Vogt, S., Woodruff, T. K., and O'Halloran, T. V. (2011) Zinc sparks are triggered by fertilization and facilitate cell cycle resumption in mammalian eggs. *ACS Chem. Biol. 6*, 716−723.
(7) Que, E. L., Bleher, R., Duncan, F. E., Kong, B. Y., Gleber, S. C., Vogt, S., Chen, S., Garwin, S. A., Bayer, A. R., Dravid, V. P., Woodruff, T. K., and O'Halloran, T. V. (2015) Quantitative mapping of zinc fluxes in the mammalian egg reveals the origin of fertilization-induced zinc sparks. *Nat. Chem. 7*, 130−139.
(8) Yamasaki, S., Sakata-Sogawa, K., Hasegawa, A., Suzuki, T., Kabu, K., Sato, E., Kurosaki, T., Yamashita, S., Tokunaga, M., Nishida, K., and Hirano, T. (2007) Zinc is a novel intracellular second messenger. *J. Cell Biol. 177*, 637−645.
(9) Taylor, K. M., Hiscox, S., Nicholson, R. I., Hogstrand, C., and Kille, P. (2012) Protein kinase CK2 triggers cytosolic zinc signaling pathways by phosphorylation of zinc channel ZIP7. *Sci. Signaling 5*, ra11.
(10) Maret, W., Jacob, C., Vallee, B. L., and Fischer, E. H. (1999) Inhibitory sites in enzymes: zinc removal and reactivation by thionein. *Proc. Natl. Acad. Sci. U. S. A. 96*, 1936−1940.
(11) Krezel, A., and Maret, W. (2008) Thionein/metallothionein control Zn(II) availability and the activity of enzymes. *J. Biol. Inorg. Chem. 13*, 401−409.
(12) Krezel, A., and Maret, W. (2007) Dual nanomolar and picomolar Zn(II) binding properties of metallothionein. *J. Am. Chem. Soc. 129*, 10911−10921.
(13) Vinkenborg, J. L., Nicolson, T. J., Bellomo, E. A., Koay, M. S., Rutter, G. A., and Merkx, M. (2009) Genetically encoded FRET sensors to monitor intracellular Zn^{2+} homeostasis. *Nat. Methods 6*, 737−740.
(14) Qin, Y., Dittmer, P. J., Park, J. G., Jansen, K. B., and Palmer, A. E. (2011) Measuring steady-state and dynamic endoplasmic reticulum and Golgi Zn^{2+} with genetically encoded sensors. *Proc. Natl. Acad. Sci. U. S. A. 108*, 7351−7356.
(15) Chabosseau, P., Tuncay, E., Meur, G., Bellomo, E. A., Hessels, A., Hughes, S., Johnson, P. R., Bugliani, M., Marchetti, P., Turan, B., Lyon, A. R., Merkx, M., and Rutter, G. A. (2014) Mitochondrial and ER-targeted eCALWY probes reveal high levels of free Zn^{2+}. *ACS Chem. Biol. 9*, 2111−2120.
(16) Maret, W. (2013) Zinc biochemistry: from a single zinc enzyme to a key element of life. *Adv. Nutr. 4*, 82−91.
(17) Hutton, J. C., Penn, E. J., and Peshavaria, M. (1983) Low-molecular-weight constituents of isolated insulin-secretory granules. Bivalent cations, adenine nucleotides and inorganic phosphate. *Biochem. J. 210*, 297−305.
(18) Linkous, D. H., Flinn, J. M., Koh, J. Y., Lanzirotti, A., Bertsch, P. M., Jones, B. F., Giblin, L. J., and Frederickson, C. J. (2008) Evidence that the ZNT3 protein controls the total amount of elemental zinc in synaptic vesicles. *J. Histochem. Cytochem. 56*, 3−6.
(19) Ho, L. H., Ruffin, R. E., Murgia, C., Li, L., Krilis, S. A., and Zalewski, P. D. (2004) Labile zinc and zinc transporter ZnT4 in mast cell granules: role in regulation of caspase activation and NF-kappaB translocation. *J. Immunol. 172*, 7750−7760.
(20) Domaille, D. W., Que, E. L., and Chang, C. J. (2008) Synthetic fluorescent sensors for studying the cell biology of metals. *Nat. Chem. Biol. 4*, 168−175.
(21) Nolan, E. M., and Lippard, S. J. (2009) Small-molecule fluorescent sensors for investigating zinc metalloneurochemistry. *Acc. Chem. Res. 42*, 193−203.
(22) Qin, Y., Miranda, J. G., Stoddard, C. I., Dean, K. M., Galati, D. F., and Palmer, A. E. (2013) Direct comparison of a genetically encoded sensor and small molecule indicator: implications for quantification of cytosolic Zn^{2+}. *ACS Chem. Biol. 8*, 2366−2371.
(23) Bozym, R. A., Thompson, R. B., Stoddard, A. K., and Fierke, C. A. (2006) Measuring picomolar intracellular exchangeable zinc in PC-12 cells using a ratiometric fluorescence biosensor. *ACS Chem. Biol. 1*, 103−111.
(24) Lindenburg, L. H., Hessels, A. M., Ebberink, E. H., Arts, R., and Merkx, M. (2013) Robust red FRET sensors using self-associating fluorescent domains. *ACS Chem. Biol. 8*, 2133−2139.
(25) Miranda, J. G., Weaver, A. L., Qin, Y., Park, J. G., Stoddard, C. I., Lin, M. Z., and Palmer, A. E. (2012) New alternately colored FRET sensors for simultaneous monitoring of Zn^{2+} in multiple cellular locations. *PLoS One 7*, e49371.
(26) Lanquar, V., Grossmann, G., Vinkenborg, J. L., Merkx, M., Thomine, S., and Frommer, W. B. (2014) Dynamic imaging of cytosolic zinc in Arabidopsis roots combining FRET sensors and RootChip technology. *New Phytol. 202*, 198−208.
(27) Bellomo, E. A., Meur, G., and Rutter, G. A. (2011) Glucose regulates free cytosolic Zn^{2+} concentration, Slc39 (ZiP), and metallothionein gene expression in primary pancreatic islet beta-cells. *J. Biol. Chem. 286*, 25778−25789.
(28) Qin, Y., Dittmer, P. J., Park, J. G., Jansen, K. B., and Palmer, A. E. (2011) Measuring steady-state and dynamic endoplasmic reticulum and Golgi Zn^{2+} with genetically encoded sensors. *Proc. Natl. Acad. Sci. U. S. A. 108*, 7351−7356.
(29) Park, J. G., Qin, Y., Galati, D. F., and Palmer, A. E. (2012) New sensors for quantitative measurement of mitochondrial Zn^{2+}. *ACS Chem. Biol. 7*, 1636−1640.
(30) Evers, T. H., Appelhof, M. A., de Graaf-Heuvelmans, P. T., Meijer, E. W., and Merkx, M. (2007) Ratiometric detection of Zn(II) using chelating fluorescent protein chimeras. *J. Mol. Biol. 374*, 411−425.
(31) Vinkenborg, J. L., van Duijnhoven, S. M., and Merkx, M. (2011) Reengineering of a fluorescent zinc sensor protein yields the first genetically encoded cadmium probe. *Chem. Commun. 47*, 11879−11881.
(32) Krizek, B. A., Zawadzke, L. E., and Berg, J. M. (1993) Independence of metal binding between tandem Cys2His2 zinc finger domains. *Protein Sci. 2*, 1313−1319.
(33) Yang, F., Moss, L. G., and Phillips, G. N., Jr. (1996) The molecular structure of green fluorescent protein. *Nat. Biotechnol. 14*, 1246−1251.
(34) Taylor, K. M., Morgan, H. E., Smart, K., Zahari, N. M., Pumford, S., Ellis, I. O., Robertson, J. F., and Nicholson, R. I. (2007) The emerging role of the LIV-1 subfamily of zinc transporters in breast cancer. *Mol. Med. 13*, 396−406.

DOI: 10.1021/acschembio.5b00211
ACS Chem. Biol. XXXX, XXX, XXX−XXX

(35) Taylor, K. M., Vichova, P., Jordan, N., Hiscox, S., Hendley, R., and Nicholson, R. I. (2008) ZIP7-mediated intracellular zinc transport contributes to aberrant growth factor signaling in antihormone-resistant breast cancer Cells. *Endocrinology 149*, 4912−4920.
(36) McCranor, B. J., Bozym, R. A., Vitolo, M. I., Fierke, C. A., Bambrick, L., Polster, B. M., Fiskum, G., and Thompson, R. B. (2012) Quantitative imaging of mitochondrial and cytosolic free zinc levels in an in vitro model of ischemia/reperfusion. *J. Bioenerg. Biomembr. 44*, 253−263.
(37) Xue, L., Li, G., Yu, C., and Jiang, H. (2012) A ratiometric and targetable fluorescent sensor for quantification of mitochondrial zinc ions. *Chem. - Eur. J. 18*, 1050−1054.
(38) Mitchell, K. J., Pinton, P., Varadi, A., Tacchetti, C., Ainscow, E. K., Pozzan, T., Rizzuto, R., and Rutter, G. A. (2001) Dense core secretory vesicles revealed as a dynamic Ca^{2+} store in neuroendocrine cells with a vesicle-associated membrane protein aequorin chimaera. *J. Cell Biol. 155*, 41−51.
(39) Knowlden, J. M., Hutcheson, I. R., Jones, H. E., Madden, T., Gee, J. M., Harper, M. E., Barrow, D., Wakeling, A. E., and Nicholson, R. I. (2003) Elevated levels of epidermal growth factor receptor/c-erbB2 heterodimers mediate an autocrine growth regulatory pathway in tamoxifen-resistant MCF-7 cells. *Endocrinology 144*, 1032−1044.
(40) Edelstein, A., Amadai, N., Hoover, K., Vale, R., and Stuurman, N. (2010) *Computer Control of Microscopes using μManager*, (Ausubel, F. M., Ed.) John Wiley & Sons, Inc., New York.
(41) Schneider, C. A., Rasband, W. S., and Eliceiri, K. W. (2012) NIH Image to ImageJ: 25 years of image analysis. *Nat. Methods 9*, 671−675.

DOI: 10.1021/acschembio.5b00211
ACS Chem. Biol. XXXX, XXX, XXX−XXX